drugs and drug candidates

MDPI

Article

The Analysis of the PI3K-AKT-mTOR Pathway and Mitochondria Modulation by a 2-Aminopyridine Compound Using the Metastatic Prostate Cancer Cell Line PC-3

Talita Alvarenga Valdes [1,2], Sabrina Mendes Botelho [1], Keli Lima [3], Carlos Alberto Montanari [4], João Agostinho Machado Neto [3,*] and Andrei Leitão [1,2,*]

[1] Chemical Discovery Group (CDG), São Carlos Institute of Chemistry (IQSC), University of São Paulo (USP), São Carlos 13566-590, Brazil; talitavaldes@gmail.com (T.A.V.); sabrina.botelho@usp.br (S.M.B.)
[2] Interunit Bioengineering Graduate Program (PPGIB), University of São Paulo (USP), São Carlos 13566-590, Brazil
[3] Department of Pharmacology, Biomedical Sciences Institute, University of São Paulo (USP), São Paulo 05508-000, Brazil
[4] Medicinal & Biological Chemistry Group (NEQUIMED), São Carlos Institute of Chemistry (IQSC), University of São Paulo (USP), São Carlos 13566-590, Brazil; carlos.montanari@usp.br
* Correspondence: jamachadoneto@usp.br (J.A.M.N.); andleitao@iqsc.usp.br (A.L.)

Abstract

Background: Prostate cancer is one of the most prevalent and deadly neoplasias in the male population. Despite the availability of therapies that increase the long-term survival of patients with localized tumors, metastatic prostate cancer is challenging to treat. A previous study revealed that the 2-aminopyridine derivative (named Neq0440) inhibited the PI3K-AKT-mTOR pathway and presented selective cytotoxicity toward the metastatic prostate cancer cell line PC-3. **Methods:** Here, we further analyzed the mechanism of action of these molecules by using cell-based colorimetric, fluorometric, epifluorescence microscopy, and Western blot assays. **Results:** Mitochondrial depolarization increased the AMPK level at 24 h inhibition with Neq0440, which led to the PI3K-AKT-mTOR pathway downregulation after 48 h. The phosphorylation was inhibited for AKT and the downstream quinases (S6RP and 4EBP1) from the PI3K-AKT-mTOR pathway, which can work together with the mitochondrial depolarization, lowering the pH of the medium, increasing ROS levels, and translocating the lysosomes toward the nucleus to trigger cell death. **Conclusions:** Therefore, Neq0440 can be used as a lead compound to obtain derivatives with a novel anticancer mechanism of action.

Keywords: cell-based assays; mechanism of action; AMPK activity; ROS formation; kinase modulation; lysosome modulation

Check for updates

Academic Editors: Jean Jacques Vanden Eynde and Marco Bruno Luigi Rocchi

Received: 5 January 2026
Revised: 24 February 2026
Accepted: 26 February 2026
Published: 2 March 2026

Copyright: © 2026 by the authors. Licensee MDPI, Basel, Switzerland. This article is an open access article distributed under the terms and conditions of the Creative Commons Attribution (CC BY) license.

1. Introduction

The prostate is an exocrine gland that comprises the male reproductive system. It is located below the bladder and in front of the rectum in the lower abdomen. Factors contributing to prostate cancer development include genetics, increased life expectancy, and unhealthy lifestyle habits [1].

Prostate cancer (PC) is a global public health problem affecting men worldwide. It is the most frequently diagnosed disease in the male population in 112 countries/territories out of 185 [2]. The incidence and mortality are correlated with age, especially above 60 years [3].

Treatment depends on tumor classification and may involve surgical removal, radiation therapy, hormone therapy, and chemotherapy [4].

Drugs administered for prostate cancer treatment may not lead to tumor elimination or disease cure. Nevertheless, they prolong patients' lives and can improve their quality of life when combined with other therapies [5]. Although chemotherapy presents promising results for prostate cancer treatment, resistance is one of the main problems [6]. Therefore, the search for new therapeutic approaches is a continuous field of study. In this sense, PI3K-AKT-mTOR pathway inhibitors are being studied, including the clinical phase candidates apitolisib (the PI3K/mTOR competitive inhibitor), capivasertib and ipatasertib (AKT competitive inhibitors) [7].

A previous cell-based study by our group demonstrated that 2-aminopyridine derivatives inhibited the PI3K-AKT-mTOR signaling pathway, with cytotoxic activity against the metastatic prostate cancer cell line PC-3 [8]. A previous hypothesis indicated that these 2-aminopyridines could inhibit the mammalian target of rapamycin (mTOR) kinase because of their chemical similarity to the potent and selective mTOR inhibitor XL388 [9]. The PI3K-AKT-mTOR signaling pathway has been linked to prostate cancer; therefore, attracting many studies in the field [10,11]. Here, the mechanism of action was elucidated for Neq0440 (Figure 1) against the prostate cancer cell line (PC-3) to evaluate its antineoplastic effects and selectivity in comparison with the non-tumoral prostate cells (PNT-2).

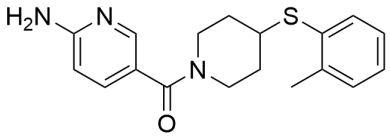


Figure 1. Chemical representation of Neq0440.

2. Results

The results are presented in sections detailing the bioactivity profiling of Neq0440, which provides a putative mechanism of action for this chemical compound.

2.1. Cytotoxicity Assays

Neq0440 was tested against bone metastatic prostate cancer (PC-3) and epithelial prostate (PNT-2) cell lines via the MTT method (Table 1 and Figure S2) [10]. As expected, Neq0440 had the same potency as previously described for PC-3 [8] and was selective toward prostate cancer cells (SI > 1). The cytotoxicity of Neq0440 against another metastatic prostate cancer (DU145) was too low (IC_{50} > 100 µM to be considered for further assays, confirming our previous assay [8]. Hence, the studies continued using PC-3 and PNT-2 cells.

Table 1. Potency (IC_{50}) and selectivity index (SI) after 72 h of incubation against prostate cancer (PC-3) and epithelial prostate (PNT-2) cell lines for Neq0440 and doxorubicin alone or combined.

Sample	$IC_{50\ PNT\text{-}2}$ ± SE (µM)	$IC_{50\ PC3}$ ± SE (µM)	SI
Neq0440	>250	65.4 ± 8.68	>3.8
Doxorubicin	0.12 ± 0.01	1.13 ± 0.18	0.11
Dox + Neq0440 [1]	0.21 ± 0.02	0.57 ± 0.11	0.37

[1] The combination comprised a set of concentrations of doxorubicin (Dox) + 1.0 µM Neq0440. SE: standard error; selectivity index (SI) = $IC_{50\ PNT\text{-}2}/IC_{50\ PC\text{-}3}$; SI > 1: selective toward the cancer cell; SI ≈ 1: no selectivity; SI < 1: selective toward the nontumoral cell.

Doxorubicin is not a chemotherapeutic drug for prostate cancer, but it can trigger reactive oxygen species that also target mitochondria in cells [11]; hence, it was also tested (Table 1). Ultimately, the mitochondrial activity could be linked with the mode of action for Neq0440, as described in the next section.

Moreover, our in-house test for doxorubicin combined with Neq0440 in triple-negative breast cancer cells revealed an eight-fold improvement in the cytotoxic response (unpublished results). Therefore, we tested whether the combination of Neq0440 at an inactive concentration of 1.0 μM with a set of doxorubicin concentrations could induce differential sensitivity toward prostate cancer cells in an exploratory approach. The results (Table 1) showed that the combination could cause differential sensitization of PC-3 cancer cells compared with non-tumoral PNT-2. The result was not striking, according to the highest single agent approach [12], but the combination of Neq0440 and doxorubicin reduced the unfavorable selectivity index. More studies will be necessary for an in-depth evaluation of the combination index.

2.2. Analysis of Mitochondrial Function

The half-maximal concentration of Neq0440 was used with a mitochondrial marker (MitoPotential) to analyze the state of these organelles inside the cells (Table 2, Figures 2 and S3). The positive control was composed of doxorubicin at 1.0 μM (near the IC_{50} for PC-3) or 10 μM (where more than 90% cell death was observed for PC-3 via the MTT assay). PC-3 and PNT-2 cells were stained after 72 h of incubation, and images were collected with the epifluorescence microscope.

Table 2. Mitochondrial potential quantification with Red/Green MitoPotential reagent against nontumoral (PNT-2) and prostate cancer cells (PC-3) after 72 h of incubation.

MitoPotential Quantification						
Samples	**CTCF (PNT-2)**			**CTCF (PC-3)**		
	Polarized (Red)	**Depolarized (Green)**	**Ratio (Red/Green)**	**Polarized (Red)**	**Depolarized (Green)**	**Ratio (Red/Green)**
Neg. Control	154,298	78,007	1.97	108,307	68,115	1.59
Neq0440 65.4 μM	165,926	90,390	1.83	186,067	164,861	1.12
Dox 1.0 μM [1]	190,854	139,255	1.37	156,648	177,272	0.88
Dox 10 μM	-	-	-	416,210	857,987	0.48

[1] Dox: doxorubicin. CTCF: amount of fluorescence from the cells/total area of the cells in the field (n = 2). A ratio (red/green) > 1.0 corresponds to functional mitochondria. A ratio (red/green) < 1.0 indicates that depolarized mitochondria can trigger cell death.

The functional mitochondria were labeled in red, and the depolarized mitochondria (with loss of membrane potential) were green. The corrected total cell fluorescence (CTCF) corresponded to the amount of fluorescence from the area divided by the total number of cells (Table 2 and Figure S4). The CTCF ratio (red/green) reflects the relationship between functional and depolarized mitochondria: (i) cells with healthy mitochondria had a score above 1, and (ii) cells with depolarized mitochondria had a score below 1 and could trigger the death process.

The PC-3 cell line had the characteristic elongated morphology with many polarized (active) mitochondria (red/green = 1.59) in the negative control wells (Figure 2a and Table 2). PNT-2 cells are naturally rounder than PC-3 cells, with a high ratio of polarized/depolarized mitochondria (red/green = 1.97), indicating healthy cells.

The positive controls made with doxorubicin at 1.0 and 10 μM led to cell rounding and mitochondria depolarization of the PC-3 cells (red/green ratio = 0.88 and 0.48, respectively) in a concentration-response relationship. As expected, the highest concentration of doxorubicin (10 μM) induced extensive cell death, which was considered too harsh to be useful for further consideration. Therefore, doxorubicin at 1.0 μM was chosen for additional assays with PNT-2 cells. The detachment of PNT-2 cells and reduction in mitochondrial polarization (red/green ratio = 1.37) were promoted by doxorubicin (Figure 2b and Table 2).

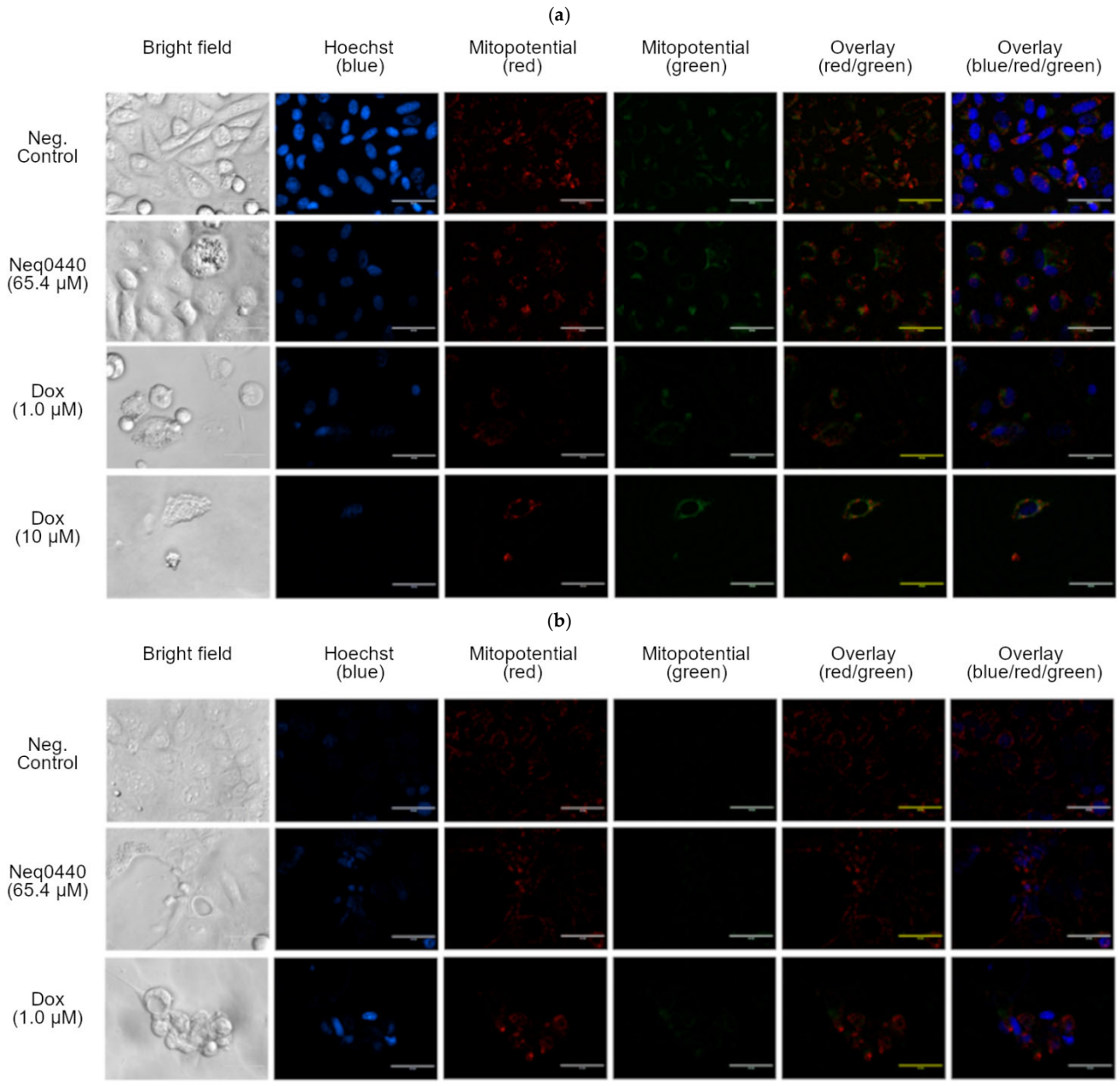


Figure 2. Morphology and the mitochondrial membrane potential of PC-3 (**a**) and PNT-2 (**b**) cells after 72 h of incubation with Neq0440 and doxorubicin (Dox). The cell morphology was analyzed using bright-field microscopy. The cell constituents were labeled blue with Hoechst 33452 (nuclei) and red/green with MitoTracker (polarized/depolarized mitochondria). Neg. Control: negative control. The white bar represents 50 µm. No image edition was made. The details can be found in Figure S3.

Neq0440 compound induced round morphology and the presence of several vacuoles in the cytoplasm of the PC-3 cells. Cytoplasmic vacuolation can occur in various cellular compartments via different mechanisms and is often associated with cell death [13]. Among the stimuli that lead to vacuole formation, exposure to chemical agents is one of the leading causes [14]. The nuclei of the PC-3 cells presented chromatin fragmentation, which may represent an advanced cell death process with genetic material damage. Rounded cells with reduced cytoplasmic content and some nuclei with DNA condensation were also observed. Although the compound was cytotoxic to PC-3 cells and caused morphological changes, the number of functional mitochondria was still higher than that of the depolarized

mitochondria (red/green ratio = 1.12). These findings indicated that the activity of the compound did not solely depend on mitochondrial alterations.

PNT-2 cells treated with the compound Neq0440 had a higher population of polarized mitochondria than that of depolarized mitochondria (Table 2, Figure 2b). This assay corroborated the MTT results, as Neq0440 was selective for PC-3 cells and inactive against PNT-2 cells.

2.3. Studying the Mechanism of Action Using Western Blot

Partial mitochondrial depolarization may trigger cell death via the canonical activation of 5′ AMP-activated protein kinase (AMPK) [15]. Hence, it was analyzed by Western blotting, along with the PI3K-AKT-mTOR pathway (Figures 3 and S3). As expected, the p-AMPK and AMPK concentrations arose after 24 h incubation, being the most pronounced alteration observed in this timeframe. The PI3K-AKT-mTOR pathway was also affected by Neq0440 at 24 h to a lower extent, showing reduced phosphorylation of AKT, mTOR, and the downstream S6RP and 4EBP1. Therefore, the mitochondrial stress that elevated AMPK level led to the inhibition of the PI3K-AKT-mTOR pathway after 48 h, where the ratio of phosphorylated kinases (except mTOR) was reduced when the IC_{50} concentration was used (Figures 3 and S3).

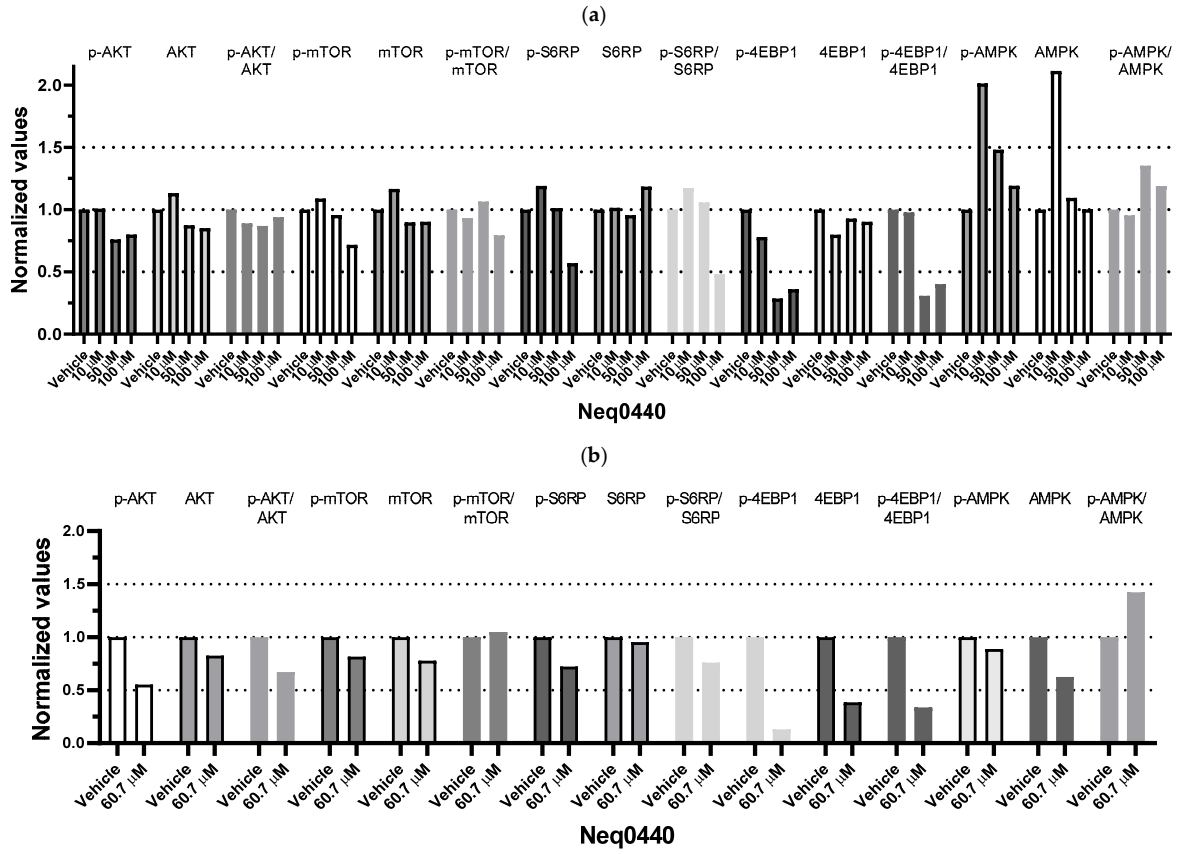


Figure 3. Quantification of the Western blot data and the ratio of phosphorylated versus total amount of kinase for compound Neq0440 was normalized using the non-treated cells after 24 h (**a**) and 48 h (**b**) of treatment.

2.4. Reactive Oxygen Species (ROS) Formation

The PI3K-AKT-mTOR pathway may control the level of intracellular reactive oxygen species (ROS) [16]. Moreover, the mitochondrial stress promoted by Neq0440 can increase ROS formation. Hence, ROS formation was quantified in PC-3 and PNT-2 cell lines treated with Neq0440 and doxorubicin (Figure 4 and Table 3). Doxorubicin is known to increase the amount of ROS inside PC-3 cells [17]. The analyses were performed for short, middle, and

prolonged exposure intervals (24, 48, and 72 h, respectively). The culture medium with 0.5% DMSO was used as a negative control, and hydrogen peroxide (H_2O_2) at a concentration of 500 µM was used as a positive control. The graph shown in Figure 4 represents the percentage of ROS over time, where the negative control corresponds to 100%.

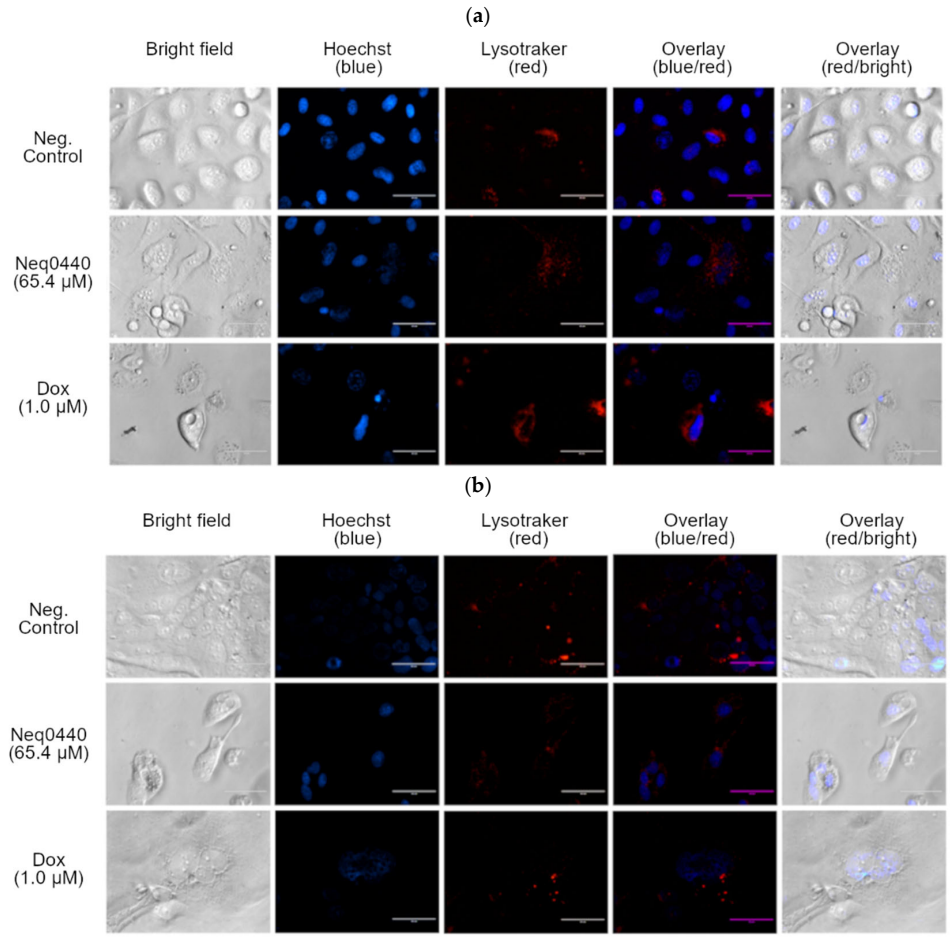


Figure 4. Morphological aspects and fluorescence markers of the nucleus and lysosomes of PC-3 (**a**) and PNT-2 (**b**) cells after 72 h of incubation with Neq0440 and doxorubicin. The negative control contained the culture medium supplemented with 0.5% (*v*/*v*) DMSO. Hoechst 33342 (blue) and LysoTracker (red) labeled nuclei and lysosomes, respectively. Scale bars represent 50 µm. No image edition was made. Details can be identified in Figure S6.

Table 3. Reactive oxygen species level in PC-3 and PNT-2 cells after 48 h treatment with Neq0440 or doxorubicin.

Samples	Relative ROS Response to Negative Control (%)								
	24 h			48 h			72 h		
	PC-3	PNT-2	Ratio [1]	PC-3	PNT-2	Ratio [1]	PC-3	PNT-2	Ratio [1]
Neq0440 65.4 µM	65.9	44.2	0.67	150	123	0.82	64.2	50.8	0.79
Dox 1.0 µM	90.9	76.7	0.84	113	108	0.95	108	67.8	0.62
Dox 10 µM	96.0	63.8	0.66	1523	77	0.50	99.4	52.7	0.53

[1] Ratio (PNT-2/PC-3) < 1: increased ROS formation in the prostate cancer cell line (PC-3); ratio > 1: increased ROS formation in the nontumoral cell line (PNT-2). $n = 2$.

Neq0440 did not induce ROS in PC-3 cells after short-term exposure (24 h). However, ROS level spiked in PC-3 cells after 48 h of exposure to Neq0440 and doxorubicin (Table 3). After a 72 h interval, there was a reduction in ROS formation for all treatments due to cell death. ROS formation was higher in PC-3 cancer cells than in non-tumoral PNT-2 prostate cells (Table 3).

2.5. Location and Quantification of the Lysosomes

Active AMPK may also work via the non-canonical pathway to modulate lysosomes [15]. Therefore, the lysosomes were labeled with the LysoTracker marker after 72 h of incubation with Neq0440 or doxorubicin at the half-maximal concentration (Figure 4 and Table 4). Opposite effects were identified for Neq0440 and doxorubicin in terms of the percentage of lysosomes relative to the negative control (untreated cells). Higher lysosomal concentration was observed in cells with more aberrant morphological changes triggered by Neq0440, where lysosomes were more evident in larger cells. The addition of Neq0440 induced lysosome accumulation around the nucleus. Small vesicles dispersed in the cytoplasm or near the cell membrane were observed in several cells, which may be related to the processes of recycling and degrading molecules.

Table 4. Quantification of the lysosome marker LysoTracker in tumoral (PC-3) and nontumoral (PNT-2) prostate cell lines after 72 h incubation with Neq0440 or doxorubicin treatment in PC-3 and PNT-2 cells.

Samples	LysoTracker Quantification				
	PNT-2		PC-3		CTCF Ratio (PNT-2/PC-3)
	CTCF	% Lysosomes [1]	CTCF	% Lysosomes [1]	
Neg. Control	83,992.13	100	117,724.38	100	0.71
Neq0440 65.4 µM	181,477.90	216	129,859.07	110	1.39
Dox 1.0 µM	135,939.77	61	465,620.60	395	0.29

[1] % lysosomes: relative percentage of lysosomes inside the cells compared with the negative control (100%). Dox: doxorubicin. CTCF: amount of fluorescence from the cells/total area of the cells in the field (n = 2). A ratio of CTCF (PNT-2/PC-3) < 1.0 indicates that the lysosomal population is high in cancer cells. A ratio of CTCF (PNT-2/PC-3) > 1.0 indicates a greater lysosomal population in PNT-2 cells.

Doxorubicin had the opposite effect on the two cell lines, decreasing the lysosomal population in PNT-2 cells and sharply increasing it in PC-3 cells (Figures 4, S6 and S7, Table 4). Lysosomes were more concentrated in cells with vacuoles, indicating their high activity.

3. Discussion

Our current data revealed that the 2-aminopyridine derivative Neq0440 had the same profile in terms of the previously described cytotoxicity [8] (Table 1), with downstream effects on the PI3K-AKT-mTOR-S6 pathway according to cell-based assays. The link between the previous identification of PI3K-AKT-mTOR pathway inhibition and the putative target was based on the observation of the pH of the culture medium, which is a phenotypic indication of altered cell metabolism. PC-3 prostate cancer cells have increased use of anaerobic metabolism, which also affects the pH of the extracellular medium [18], indicating mitochondrial stress. The empirical observation of the pH reduction caused by Neq0440 incubation with PC-3 cells provided indirect evidence that mitochondrial metabolism could be further affected. Hence, the MitoPotential reagent was used to quantify mitochondrial function after treatment. The mitochondria were more depolarized in PC-3 prostate cancer cells than the non-tumoral PNT-2 cells after Neq0440 treatment (Table 2), which indicates that the cancer cells were more sensitive. This result can also help explain the selective cytotoxicity of Neq0440 toward PC-3 cells (Table 1). Doxorubicin, a known anticancer drug, was used as a positive control for these assays because it led to cell death via interaction with topoisomerase II, the formation of ketone bodies, and the generation of ROS [17]. Some of these characteristics were observed in Figure 2, especially after treatment with 1.0 µM of doxorubicin.

The mitochondrial stress caused by oxygen deprivation and nutrient deficiency decreases ATP levels and increases ROS levels. Reactive oxygen species also influence mitochondrial function and mediate intracellular calcium levels to activate programmed cell

death, as previously described for the prostate cancer PC-3 cell line [19]. As expected, doxorubicin led to mitochondrial depolarization to a greater extent than Neq0440.

ATP consumption also increases the AMP/ADP intracellular concentration that activates AMPK, resulting in protein phosphorylation [15]. Interestingly, AMPK levels increased at 24 h, but the ratio p-AMPK/AMPK increased only after 48 h incubation with Neq0440 (Figure 3 and Figure S5). Higher levels of p-AMPK can also modulate the PI3K-AKT-mTOR pathway. The reduction in the intermembrane potential was lower for the non-tumoral PNT-2 cells, showing selectivity for the PC-3 lineage (Table 2). These findings indicate that the mitochondria in PNT-2 cells were more resistant to the treatment than those in PC-3 cells for Neq0440 treatment.

Lysosomes produce large amounts of amino acids under the condition of nutritional balance. However, nutrient deficiency triggers the movement of proteins involved in lysosome movement toward the nucleus [20]. In addition, lysosomes interact with mitochondria and the endoplasmic reticulum for homeostatic regulation [19], which can also be affected by the mitochondrial stress promoted by the treatment. The location of the lysosomes around the nucleus may indicate metabolic stress. The metabolic stress caused by Neq0440 treatment kept the lysosomes close to the nucleus in PC-3 cells (Figure 4), reinforcing nutritional deprivation conditions. In addition, Neq0440 induced differential lysosome biogenesis in favor of non-tumoral cells. For doxorubicin, an opposite effect was observed for fibroblasts (decrement) and prostate cancer cells (increment), which can be linked to the higher cytotoxicity of this chemical against the former cell line.

The Western blot results provided a clear picture of the Neq0440 bioactivity against the PC-3 cells (Figures 3 and S5). Neq0440 downregulated the PI3K-AKT-mTOR pathway via the high AMPK level from mitochondrial stress. It is important to note that EBP1 and S6RP are linked to the development of prostate cancer, and the PC-3 lineage presents high levels of these kinases that were inactivated by Neq0440 [21,22].

Finally, it should be noted that this in vitro study brings its own limitations in terms of the in vivo physiological context. Therefore, a deeper analysis of the proposed mechanism in vivo can also provide more valuable insights.

In summary, compound Neq0440 was cytotoxic and selective against PC-3 prostate cancer cells, with a mechanism of action shown in Figure 5. The ratio of polarized versus depolarized mitochondria was reduced after 72 h of incubation in PC-3 cells, along with the pH reduction and an increase in ROS after 48 h. The mitochondrial stress elevated the AMPK level, with an inhibition of the downstream PI3K-AKT-mTOR pathway. Neq0440 could not promote lysosome biogenesis in PC-3 cells to the same extent as PNT-2 cells. Moreover, the lysosomes were located near the nucleus of the PC-3 cells after Neq0440 treatment, which also indicates metabolic stress [23]. Overall, this study improved the current knowledge of the bioactivity of this 2-aminopyridine chemical that can be used to evaluate novel derivatives in an anticancer drug discovery effort. Novel chemicals based on Neq0440 are now being studied to identify a structure-activity relationship (SAR) using the phenotypic cytotoxic response, and the results will be presented in a follow-up study.

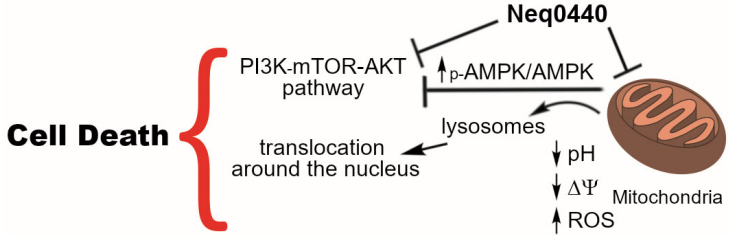


Figure 5. The proposed mechanism of action of Neq0440 in PC-3 prostate cancer cells.

4. Materials and Methods

4.1. Chemicals

Compound Neq0440 was acquired from ChemBridge Corporation, San Diego, CA, USA (12935164 and #18144428, respectively), with purity above 95%, as previously described [8]. The free-base form of doxorubicin (CAS 23214-92-8) was obtained from MedKoo Biosciences, Inc., Morrisville, NC, USA (code 100960). According to the HPLC data provided by the companies, the purity was greater than 95%.

All compounds were solubilized in DMSO at a concentration of 50 mM and stored at −20 °C. The working solutions were prepared at the desired concentrations with 0.5% (*v*/*v*) of DMSO of the stock compound diluted in the culture medium.

4.2. Cell Culture

Prostate (PNT-2) and metastatic adenocarcinoma (PC-3) cell lines were acquired from the Cell Bank of Rio de Janeiro (BCRJ), codes 0269 and 0047, respectively. The metastatic prostate carcinoma cell line PC-3, derived from bone metastasis, was cultured in F-12K medium (Cultilab®, Campinas, Brazil). The non-tumoral human prostate cell line PNT-2 was cultured in RPMI 1640 medium supplemented with 0.35% (*w*/*v*) glucose. All culture media were supplemented with 0.15% sodium bicarbonate (*w*/*v*), 10% inactivated fetal bovine serum (*v*/*v*), and 1.0% penicillin/streptomycin (*v*/*v*) solution. The cells were cultured in T75 flasks and maintained in an incubator at 37 °C, 90% humidity, and 5% CO_2 until they reached 80% confluence. All cells were used until passage 15.

4.3. Cell Viability Assay

The cells were seeded at a concentration of 1.0×10^4 cells/well (100 µL at 1.0×10^5 cells/mL) in 96-well plates, followed by 24 h of incubation for adhesion. The compounds were then pipetted into each well and incubated at 37 °C and 5% CO_2 for 72 h. Culture medium supplemented with 0.5% (*v*/*v*) DMSO was used as a negative control. Doxorubicin (Dox) was administered as a positive control for cell death. The viability was measured after 3 h of incubation with MTT at a concentration of 1.0 mg/mL [8]. The absorbance was quantified at 570 nm with a Biobase plate reader (BIOBASE Group, Jinan, China). All analyses were performed in quintuplicate with two independent assays. The same method was used to determine the IC_{50}. Cell viability was evaluated for all compounds at concentrations of 1.0, 10, 33.3, 66.6, 100, 150, and 250 µM. The selectivity index (SI) of these substances was determined by considering the ratio between the IC_{50} values of the nontumoral cell and the cancer cell, with higher selectivity indicating lower drug side effects.

The selectivity index (SI) was calculated based on the IC_{50}:

$$SI = IC_{50\ PNT\text{-}2} / IC_{50\ PC\text{-}3} \quad (1)$$

SI < 1 indicates that the treatment was more cytotoxic to non-tumoral cells. When the SI was > 1, the treatment was more cytotoxic (selective) to the prostate cancer cell line. For SI ≈ 1, there was no selectivity.

The cytotoxicity of DMSO was evaluated, and a final concentration of 0.5% (*v*/*v*) was chosen, as it was found to be inactive for PC-3 cells (Figure S1).

4.4. Combined Therapy

The cells were seeded in 96-well plates at a concentration of 1.0×10^4 cells/well and maintained at 5% CO_2 in a humidified incubator for 24 h to promote cell adhesion. The therapeutic scheme was designed for each plate containing doxorubicin at concentrations of 0.0010, 0.0030, 0.010, 0.030, 0.10, 0.33, 1.0, 10, and 100 µM (for the standalone therapy) or in combination with the inactive concentration of 1.0 µM for Neq0440. Culture medium supple-

mented with 0.5% (*v*/*v*) DMSO was used as a negative control. After 72 h, the absorbance was quantified at 570 nm via a Biotek Synergy HT plate reader (Agilent Technologies, Inc., Winooski, VT, USA). All analyses were performed in quintuplicate in two independent assays. The data are presented as percentages, and the negative control was considered 100%.

4.5. Epifluorescence Microscopy

The cells were seeded at a density of 1.0×10^4 cells/well in 96-well black plates with a crystal flat bottom (CellView™, Greiner Bio-One, Frickenhausen, Germany) and incubated in a humidified chamber at 37 °C and 5% CO_2 to promote cell adhesion to the plate surface. After 24 h, the cells were treated with test compounds and incubated for 72 h. After incubation, the wells were washed with PBS, and the fluorescent markers were added. Each reagent was prepared according to the manufacturer's instructions. The nuclei were stained with Hoechst 33,342 (λ_{exc} = 350 nm; λ_{em} = 461 nm) and detected using a DAPI cube (blue). Mitochondrial polarization was quantified with a Guava Mitochondrial Depolarization Kit (Cytek Biosciences, Inc., Fremont, CA, USA) (4500-0250) and observed at the corresponding wavelengths for JC-1 (λ_{exc} = 514 nm; λ_{em} = 529 nm) and 7-AAD (λ_{exc} = 549 nm; λ_{em} = 644 nm) via GFP (green) and Texas Red (red) cubes, respectively. LysoTracker™ (Thermo Fisher Scientific, Waltham, MA, USA) was used for red staining the lysosomes. Images of the morphological structures and fluorophores were obtained with an EVOS FL epifluorescence microscope (Thermo Fisher Scientific, USA) at 60× magnification. All steps for obtaining the images were standardized to avoid bias using the EVOS FL epifluorescence microscope. The cells were photographed with 60% illumination, and image editing was performed via FIJI/ImageJ v. 1.54 software [24]. Image standardization was achieved by subtracting the background (50.0 pixels), with contrast and brightness increasing from 0 to 70. The ratio between the fluorescence of the image area and the total number of cells provided the CTCF values. The data refer to the mean CTCF value of the assay performed in duplicate (n = 2).

4.6. Western Blot

Total protein extraction from PC-3 cells incubated for 24 h without any treatment or with graded concentrations of Neq0440 (vehicle, 10, 50, or 100 μM) was performed with buffer containing 100 mM Tris (pH 7.6), 1.0% Triton X-100, 150 mM NaCl, 2.0 mM PMSF, 10 mM Na_3VO_4, 100 mM NaF, 10 mM $Na_4P_2O_7$, and 4.0 mM EDTA. The extracted proteins were quantified via the Bradford method. Equal amounts of protein (50 μg) were used from total extracts, followed by SDS-PAGE and Western blotting analysis with the indicated antibodies as previously described [25]. The percentage of the polyacrylamide gels ranged from 8 to 15%, and nitrocellulose membranes (GE Healthcare, Chicago, IL, USA) were used. Antibodies against p-mTOR (cat. no. 2971), mTOR (cat. no. 2972), p-AKT (cat. no. 4060), AKT (cat. no. 4685), p-4EBP1 (cat. no. 9455), 4EBP1 (cat. no. 9452), p-S6RP (cat. no. 4858), S6RP (cat. no. 2217), p-AMPK (cat. no. 2535), AMPK (cat. no. 2532), and α-tubulin (cat. no. 2144) were obtained from Cell Signaling Technology, Inc. (Danvers, MA, USA). All primary antibodies used were diluted 1:2000 and incubated for 16 h. α-tubulin was used as the loading control. The secondary antibodies anti-rabbit IgG (cat. no. 7074P2) and anti-mouse IgG (cat. no. 7076P2) conjugated with horseradish peroxidase were obtained from Cell Signaling Technology, Inc. and were used at a 1:2000 dilution with a 2 h incubation. The SuperSignal™ West Dura Extended Duration Substrate system (Thermo Fisher Scientific, Inc., USA) and G:BOX Chemi XX6 gel document system (Syngene Europe, Bengaluru, India) were used for blot visualization.

4.7. Investigation of Reactive Oxygen Species (ROS) Formation

The cells were trypsinized at 80% confluence, and the cell concentration was adjusted to 1.0×10^4 cells/well in 96-well plates. The plates were incubated in a humidified chamber at 37 °C and 5% CO_2 for 24 h. After adhesion, the cells were treated with compounds of interest. The analyses were performed at 24, 48, and 72 h intervals. All the wells were washed twice with PBS, followed by incubation with DCFH-DA (500 μM in PBS) for 30 min. After all the wells were washed, the fluorescence was immediately measured via a Biotek Synergy HT plate reader (λ_{exc} = 485/40 nm and λ_{em} = 532/40 nm). The negative control consisted of culture medium supplemented with 0.5% DMSO. The positive control contained 500 μM H_2O_2. All analyses were performed in quintuplicate with two independent assays. The relative percentage was calculated from the raw data to the negative control (100% response).

4.8. Statistical Analysis

All the data were gathered and transformed via MS Excel® and analyzed with GraphPad v. 6. The values are shown as the means ± errors unless otherwise stated.

Supplementary Materials: The following supporting information can be downloaded at https://www.mdpi.com/article/10.3390/ddc5010018/s1, Figure S1. DMSO screening against PC-3 cells. Experiments were performed using MTT as described in the main text. Statistical significance using one-way ANOVA with Dunnett post-hoc study: p value < 0.001. Figure S2. Concentration-response curves for doxorubicin monotherapy and the combination therapy with Neq0440 at 1.0 μM for the PNT-2 (nontumoral) and PC-3 (tumoral) prostate cell lines. Figure S3. Morphology and the mitochondrial membrane potential of PC-3 (a) and PNT-2 (b) cells (bright-field microscopy) after 72 h incubation of Neq0440 at the IC50, and doxorubicin (Dox) at 1.0 and 10 μM. The cell constituents were labeled in blue by Hoechst 33452 (nuclei), red and green by the Mitopotential (polarized and depolarized mitochondria, respectively). Neg. control: negative control. The white bar represents 50 μm. Figure S4. MitoPotential quantification for PC-3 and PNT-2 cells after 3 days of incubation. Figure S5. Western blot analyses of the kinase phosphorylation modulation in PC-3 cells after 24 h (a) and 48 h (b) of incubation with compound Neq0440. Figure S6. Morphological aspects and the fluorescence markers of nucleus and lysosomes for the PC-3 (a) and PNT-2 (b) cells after 72 h incubation with Neq0438, Neq0440, and doxorubicin. Negative control comprised the culture medium with 0.5% (v/v) DMSO. Hoechst33342 (blue) and Lysotracker (red) labeled nucleus and lysosomes, respectively. Scale bars represent 50 μm. Figure S7. Lysotracker marker quantification after 72 h incubation of Neq0440 with PNT-2 and PC-3 cell lines. The two-way ANOVA was applied with multiple comparisons using the Dunnett test ($p < 0.05$) concerning the negative control for each cell type.

Author Contributions: A.L. and J.A.M.N. designed the project and analyzed the results. A.L., J.A.M.N. and C.A.M. provided funding. T.A.V., S.M.B. and K.L. performed all the cell-based assays. Writing—review and editing were performed by T.A.V. and A.L. All authors have read and agreed to the published version of the manuscript.

Funding: This research was funded by the São Paulo Research Foundation (FAPESP) 2020/16799-1 (S.M.B.), 2023/12246-6 (J.A.M.N.), 2023/16111-8 (A.L.); the National Research Council (CNPq) 312086/2023-7 (A.L.); and Coordenação de Aperfeiçoamento de Pessoal de Nível Superior—Brazil (CAPES)—Finance Code 001 (T.A.V.).

Data Availability Statement: The original contributions presented in this study are included in the article/Supplementary Material. Further inquiries can be directed to the corresponding authors.

Acknowledgments: All authors have reviewed and edited the output and take full responsibility for the content of this publication.

Conflicts of Interest: The authors declare no conflicts of interest.

Abbreviations

The following abbreviations are used in this manuscript:

4EBP1	Eukaryotic initiation factor 4E-binding protein 1
7-AAD	7-Aminoactinomycin D
AKT	Protein kinase B
AMPK	5′ AMP-activated protein kinase
BCRJ	Cell Bank of Rio de Janeiro
CTFC	Corrected total cell fluorescence
Dox	Doxorubicin
DMSO	Dimethyl sulfoxide
DU145	Prostate cancer cell line
HPLC	High-performance liquid chromatography
IC_{50}	Half maximal inhibitory concentration
mTOR	Mammalian target of rapamycin
MTT	3-(4,5-di methyl thiazol-2-yl)-2,5-diphenyltetrazolium bromide
PC-3	Prostate cancer cell line
PI3K	Phosphoinositide 3-kinase
PNT-2	Prostate cell line
ROS	Reactive oxygen species
S6RP	Ribosomal protein S6
SI	Selectivity index

References

1. Ng, K.L. The Etiology of Prostate Cancer. In *Prostate Cancer*; Bott, S.R., Ng, K.L., Eds.; Exon Publications: Brisbane, Australia, 2021.
2. Bergengren, O.; Pekala, K.R.; Matsoukas, K.; Fainberg, J.; Mungovan, S.F.; Bratt, O.; Bray, F.; Brawley, O.; Luckenbaugh, A.N.; Mucci, L.; et al. 2022 Update on Prostate Cancer Epidemiology and Risk Factors—A Systematic Review. *Eur. Urol.* **2023**, *84*, 191–206. [CrossRef]
3. Giona, S. The Epidemiology of Prostate Cancer. In *Prostate Cancer*; Bott, S.R., Ng, K.L., Eds.; Exon Publications: Brisbane, Australia, 2021; pp. 1–16.
4. Sekhoacha, M.; Riet, K.; Motloung, P.; Gumenku, L.; Adegoke, A.; Mashele, S. Prostate Cancer Review: Genetics, Diagnosis, Treatment Options, and Alternative Approaches. *Molecules* **2022**, *27*, 5730. [CrossRef] [PubMed]
5. Achard, V.; Putora, P.M.; Omlin, A.; Zilli, T.; Fischer, S. Metastatic Prostate Cancer: Treatment Options. *Oncology* **2021**, *100*, 48–59. [CrossRef] [PubMed]
6. Naseer, F.; Ahmad, T.; Kousar, K.; Anjum, S. Advanced Therapeutic Options for Treatment of Metastatic Castration Resistant Prostatic Adenocarcinoma. *Front. Pharmacol.* **2021**, *12*, 728054. [CrossRef] [PubMed]
7. Huang, F.; Li, K.; Shevach, J.W.; Wang, Q. Emerging therapies to overcome antiandrogen resistance and beyond in lethal prostate cancer. *J. Natl. Cancer Cent.* **2026**, *6*, 42–57. [CrossRef]
8. Saidel, M.E.; dos Santos, K.C.; Nagano, L.F.P.; Montanari, C.A.; Leitão, A. Novel anti-prostate cancer scaffold identified by the combination of in silico and cell-based assays targeting the PI3K-AKT-mTOR pathway. *Bioorg. Med. Chem. Lett.* **2017**, *27*, 4001–4006. [CrossRef]
9. Mao, B.; Zhang, Q.; Ma, L.; Zhao, D.-S.; Zhao, P.; Yan, P. Overview of Research into mTOR Inhibitors. *Molecules* **2022**, *27*, 5295. [CrossRef]
10. Wang, R.; Qu, Z.; Lv, Y.; Yao, L.; Qian, Y.; Zhang, X.; Xiang, L. Important Roles of PI3K/AKT Signaling Pathway and Relevant Inhibitors in Prostate Cancer Progression. *Cancer Med.* **2024**, *13*, e70354. [CrossRef]
11. Peng, Y.; Wang, Y.; Zhou, C.; Mei, W.; Zeng, C. PI3K/Akt/mTOR Pathway and Its Role in Cancer Therapeutics: Are We Making Headway? *Front. Oncol.* **2022**, *12*, 819128. [CrossRef]
12. Ghasemi, M.; Turnbull, T.; Sebastian, S.; Kempson, I. The MTT Assay: Utility, Limitations, Pitfalls, and Interpretation in Bulk and Single-Cell Analysis. *Int. J. Mol. Sci.* **2021**, *22*, 12827. [CrossRef]
13. Kciuk, M.; Gielecińska, A.; Mujwar, S.; Kołat, D.; Kałuzińska-Kołat, Ż.; Celik, I.; Kontek, R. Doxorubicin—An Agent with Multiple Mechanisms of Anticancer Activity. *Cells* **2023**, *12*, 659. [CrossRef] [PubMed]
14. Foucquier, J.; Guedj, M. Analysis of drug combinations: Current methodological landscape. *Pharmacol. Res. Perspect.* **2015**, *3*, e00149. [CrossRef] [PubMed]

15. Yan, G.; Elbadawi, M.; Efferth, T. Multiple Cell Death Modalities and Their Key Features (Review). *World Acad. Sci. J.* **2020**, *2*, 39–48. [CrossRef]
16. Shubin, A.V.; Demidyuk, I.V.; Komissarov, A.A.; Rafieva, L.M.; Kostrov, S.V. Cytoplasmic vacuolization in cell death and survival. *Oncotarget* **2016**, *7*, 55863–55889. [CrossRef]
17. Steinberg, G.R.; Hardie, D.G. New Insights into Activation and Function of the AMPK. *Nat. Rev. Mol. Cell Biol.* **2023**, *24*, 255–272. [CrossRef]
18. Kma, L.; Baruah, T.J. The Interplay of ROS and the PI3K/Akt Pathway in Autophagy Regulation. *Biotechnol. Appl. Biochem.* **2022**, *69*, 248–264. [CrossRef]
19. Wagner, B.A.; Evig, C.B.; Reszka, K.J.; Buettner, G.R.; Burns, C.P. Doxorubicin Increases Intracellular Hydrogen Peroxide in PC3 Prostate Cancer Cells. *Arch. Biochem. Biophys.* **2005**, *440*, 181–190. [CrossRef]
20. Higgins, L.H.; Withers, H.G.; Garbens, A.; Love, H.D.; Magnoni, L.; Hayward, S.W.; Moyes, C.D. Hypoxia and the Metabolic Phenotype of Prostate Cancer Cells. *Biochim. Biophys. Acta Bioenerg.* **2009**, *1787*, 1433–1443. [CrossRef]
21. Wong, Y.C.; Kim, S.; Peng, W.; Krainc, D. Regulation and Function of Mitochondria–Lysosome Membrane Contact Sites in Cellular Homeostasis. *Trends Cell Biol.* **2019**, *29*, 500–513. [CrossRef]
22. Zhao, Q.; Gao, S.M.; Wang, M.C. Molecular Mechanisms of Lysosome and Nucleus Communication. *Trends Biochem. Sci.* **2020**, *45*, 978–991. [CrossRef]
23. Wang, K.; Wang, K.; Ma, Q. The Expression and Significance of p4E-BP1/4E-BP1 in Prostate Cancer. *J. Clin. Lab. Anal.* **2022**, *36*, e24332. [CrossRef]
24. Schindelin, J.; Arganda-Carreras, I.; Frise, E.; Kaynig, V.; Longair, M.; Pietzsch, T.; Preibisch, S.; Rueden, C.; Saalfeld, S.; Schmid, B.; et al. Fiji: An Open-Source Platform for Biological-Image Analysis. *Nat. Methods* **2012**, *9*, 676–682. [CrossRef]
25. Lima, K.; Carlos, J.; Alves-Paiva, R.M.; Vicari, H.P.; Souza Santos, F.P.; Hamerschlak, N.; Costa-Lotufo, L.V.; Traina, F.; Machado-Neto, J.A. Reversine exhibits antineoplastic activity in JAK2(V617F)-positive myeloproliferative neoplasms. *Sci. Rep.* **2019**, *9*, 9895. [CrossRef]

Disclaimer/Publisher's Note: The statements, opinions and data contained in all publications are solely those of the individual author(s) and contributor(s) and not of MDPI and/or the editor(s). MDPI and/or the editor(s) disclaim responsibility for any injury to people or property resulting from any ideas, methods, instructions or products referred to in the content.